

Energy Consumption Model for Power Management in Wireless Sensor Networks

Qin Wang, Woodward Yang

School of Engineering and Applied Sciences

Harvard University

{qwang, woody}@eecs.harvard.edu

Abstract —It is well recognized that a proper energy consumption model is a foundation for developing and evaluating a power management scheme in the wireless sensor networks (WSN). However, by investigating the organization and behavior of the communication subsystem in WSN devices, we found that in terms of energy consumption, the actual specifications of real WSN devices are significantly different from those typically assumed while designing and evaluating the energy-aware protocols. We argue that the fundamental energy consumption behavior of real WSN devices is critically important to properly model before optimizing or developing an energy-aware design even at higher communication layers. Thus, we initially propose a general energy consumption model of WSN devices based on their actual hardware architecture. In particular, we utilize measured energy consumption performance of the actual hardware components to implement a realistic CSECM (Communication Subsystem Energy Consumption Model) of WSN devices, which reflects the energy consumption in various functioning states and during transitions between states of the devices. By applying the CSECM, we are able to evaluate and analyze the energy efficiency of various WSN sleeping schedule protocols. Experimental measurements with real WSN devices (CC1000 and CC2420) validated the CSECM and its application methodology. Furthermore, using realistic CSECM parameter from real WSN devices has significant impact on the evaluation of energy efficient WSN sleeping schedule protocols and in developing effective power management schemes.

I. INTRODUCTION

A wireless sensor network (WSN) consists of a large number of nodes. Within a WSN, nodes collaborate amongst themselves to accomplish a common task. Because nodes are usually battery-powered and operate without attendance for a relatively long period of time, energy efficiency becomes of critical importance. Therefore, in the wireless sensor network community, a significant focus has been on put on increasing energy efficiency.

Research at every layer of wireless sensor networks considers energy efficiency as a key metric. On one side, energy efficient upper layer protocols and algorithms are proposed, such as energy efficient

MAC/LLC layer (e.g. [1]), low duty cycle sleeping scheduling (e.g. [2] [3]), and energy aware routing protocol (e.g. [4]). Similarly, developers of WSN device hardware seek to provide various techniques to reduce power consumption. For example, microprocessor ATmega [13], which is widely used in the wireless sensor network devices, provides six power-saving modes, i.e. idle, power down, power save, ADC noise reduction, standby, and extended standby. In each power-saving mode, part of microprocessor is turn off. Similarly, communication subsystems, such as CC1000 [14] and CC2420 [15], also provide some power-saving states, like power down, power save, and power off. However, there has been limited work on the upper layer protocols which fully exploit these device features.

Roughly speaking, power control and power management are major technologies used in WSN for increasing energy efficiency, even though they may appear in various ways in different layers. In our previous work [5], we presented a power consumption model for the power control in WSN. This paper will focus on the energy consumption model for power management in WSN, specifically, in the communication subsystem of WSN device. The remainder of this paper is organized as follows. Section 2 describes the related work. In section 3, a communication subsystem energy consumption model (CSECM) is derived by analyzing the organization and behavior of the communication subsystem. In section 4, we take the working clock design as an example to apply CSECM, and establish the energy consumption model for two schemes; we validate CSECM by the experiments with CC1000 and CC2420. In section 5, with the parameter values from real devices, CC1000 and CC2420, we analyze the impact of the parameters in CSECM on the working clock schemes and deduce the criteria for working clock design. Section 6 concludes the paper.

II. RELATED WORK

The energy consumption of communication subsystem in the wireless sensor network device can be divided into two parts, the first part is that related

with transmitting power, and the second part is the energy consumption in the communication subsystem circuit. Most of energy consumption models focus on the first part, while it is assumed that the second part of power consumption is constant. Ref [6] proposed the following model for estimating the power consumption of the communication subsystem.

$$E_T(d) = \begin{cases} E_{T_dec} + \epsilon_{\beta} \times d^2, & d < d_0 \\ E_{T_dec} + \epsilon_{mp} \times d^4, & d \geq d_0 \end{cases}$$

$$E_R = E_{R-elec}$$

Where, the path loss exponent includes 2 and 4, $E_{T-elec} = E_{R-elec} = E_{elec} = 50\text{nJ/bit}$, and $\epsilon_{\beta} = 10\text{pJ/bit/m}^2$, and $\epsilon_{mp} = 0.0013\text{pJ/bit/m}^4$.

In our previous research on power consumption model of device, we take the feature of power amplifier (PA) into consideration, and then propose the following model for estimating the power consumption [5].

$$P_r(d) = P_{R0} + \frac{P_{Rx} \times A \times d^\alpha}{\eta}$$

$$P_R = P_{R0}$$

Where $P_{Rx} \times A \times d^\alpha$ is the power delivered to the antenna by the PA of the transmitting node, in which P_{Rx} is the power received by the antenna of receiving node and delivered to the low noise amplifier (LNA); A is determined by characteristics of the transmitting and receiving antennas; path loss exponent is given by α . The parameter η is the drain efficiency of PA. P_{R0} and P_{Rx} are constant, and denote the power consumption in the circuit.

Actually, it is well known that when we concern the total energy consumption in the whole lifetime of sensor network devices, instead of only the process of transmitting and receiving data, the energy consumption in the circuit varies significantly depending on the state, on which the device is running. From the view of upper layer protocol/algorithm, the communication subsystem is usually assumed to have four states, i.e. *Transmitting, Receiving, idle listening and sleeping* [2] and no cost for transitions between states. Some researchers try to take more realistic factors into consideration, e.g. ref [7] defines more than the four states, i.e. *Tx, Rx, Overhearing, Idle, Sensing, and Sleeping*; ref. [8] takes the energy consumption during the transitions among states into consideration. Ref. [9] presents the energy consumption measurement in the steady states and during transitions for CC2420, in which four states, i.e. *shutdown, idle, transmit, and receive*, are included.

However, even though the researches, e.g. [7][8][9] begin to formula the energy consumption while re-thinking the states of WNS nodes and the energy consumption both in the steady states and during the transitions, few papers provide a clear mapping between upper layer assumption of device and the feature of communication subsystem in real devices.

We believe that the energy consumption model should be a function of the features of devices. Thus, in this paper, we derive the energy consumption model from the hardware structure and behavior. In addition, we verify the result through the experiment with real device.

III. ENERGY CONSUMPTION MODEL OF COMMUNICATION SUBSYSTEM

Noticing the common features of commercial products, e.g. [14] [15], and academic solutions, e.g. [10] [11], we derive the communication subsystem energy consumption model (CSECM) for power management in the WSN in four steps. Firstly, a general structure of the communication subsystem is extracted. Secondly, its state transition mechanism is derived. Thirdly, the energy consumption of the communication subsystem is parameterized. Finally, the CSECM is established based on the energy consumed in each state and transition between states.

A. General Structure of Communication Subsystem

By investigating the current solutions, i.e. [14] [15] [10] [11], it is found that the communication subsystem usually includes six sub-modules (Figure 1(a)), which mainly affect the energy consumption model, i.e. receiving module (Rx), transmitting module (Tx), voltage regulator (VR), crystal oscillator (XOSC), bias generator (BG), and frequency synthesizer (FS). Depending on implementation, those sub-modules may be integrated into a chip (e.g. CC2420), or partly integrated into a chip and remained parts on the PCB board (e.g. CC1000).

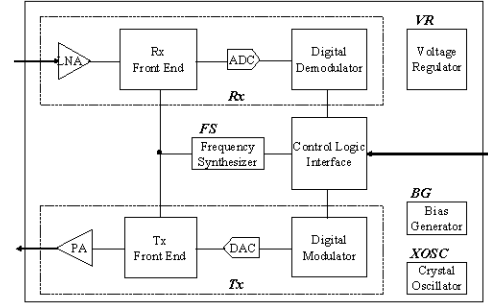


Figure 1(a). Block Diagram of Communication Sub-system

B. State Machine of Communication Subsystem

From the function and behavior of the six sub-modules, we deduce the state machine of the communication subsystem (Figure 1(b)). There are five states, i.e. *Power Off, Power Down, Power Save, Rx, and Tx*. The statements in the boxes show the actions on some sub-modules during a transition. For example, from *Power Off* to *Power Down*, the sequence of operation includes turning on VR, turning on XOSC, then calibrating FS initially, and turning off XOSC

after the initial calibration.

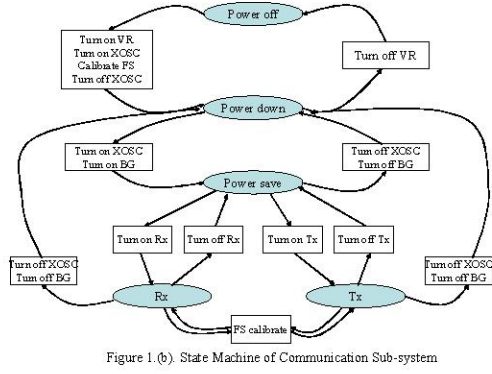


Figure 1.(b). State Machine of Communication Sub-system

Table-1. Parameterization of the communication subsystem energy consumption

Current para.	Interval para.	Sub-module Status/action					
		VR	FS	XOSC	BG	Rx	Tx
I _{off}	T _{off}	off	No-calibrated	Off	Off	Off	Off
I _{down}	T _{down}	on	Initial Calibrated	Off	Off	Off	Off
I _{save}	T _{save}	on	Initial Calibrated	On	On	Off	Off
I _{rx}	T _{rx}	on	Calibrated for Rx	On	On	On	Off
I _{tx}	T _{tx}	on	Calibrated for Tx	On	On	Off	On
I _{off_down}	T _{off_down}	Off=>on	Initial Calibrate	Off	Off	Off	Off
I _{down_save}	T _{down_save}	on	Initial Calibrated	Off=>on	Off=>on	Off	Off
I _{save_rx}	T _{save_rx}	on	Calibrate for Rx	On	On	Off=>on	Off
I _{save_tx}	T _{save_tx}	on	Calibrate for Tx	On	On	Off	Off=>on
I _{tx_rx}	T _{tx_rx}	on	Calibrate for Rx	On	On	Off=>on	Off
I _{rx_tx}	T _{rx_tx}	on	Calibrate for Tx	On	On	Off	Off=>on

Where, I_{xxx} denotes the current in the state xxx; T_{xxx} denotes the interval in the state xxx; I_{xxx_yyy} denotes the current in the process from state xxx to state yyy. T_{xxx_yyy} denotes the interval from state xxx to state yyy.

D. CSECM

Based on the definition of general structure, state machine, and the parameterization, we propose the energy consumption model (CSECM) as follows. Assume {S(1); S(2); ...; S(n)} is the state sequence of device in a given period, V_{S(k)} and V_{S(k)_S(k+1)} denotes voltage in the state S(k) and during the transition from S(k) to S(k+1), respectively. Then, the energy consumption of the device during the period, E_D, is,

$$E_D = \sum_{k=1}^n T_{S(k)} \times V_{S(k)} \times V_{S(k)} + \sum_{k=0}^{n-1} T_{S(k)_S(k+1)} \times I_{S(k)_S(k+1)} \times V_{S(k)_S(k+1)} \quad (1)$$

Where,

$$S(k) \in \{Power_Off, Power_down, Power_save, Tx, Rx\}$$

The first part of E_D is the energy consumed in the steady states; and the second part of E_D is the energy consumed during the transitions between states. Because of the continuous of the states in a device, the first transition should be from the last state of the previous period to the first state of the current period.

C. Parameterization

By comparing the general structure and state machine of communication subsystem with the current designs, e.g. [14] [15] [10] [11], it is obvious that the detail of operation sequence for each transition may be various. However, because what we concern is the energy consumption of the communication subsystem, we can parameterize the communication subsystem in terms of current and interval in the steady state and transition, regardless the detail of operations included in the steady state and transition. Table-1 shows the parameterization of the energy consumption of communication subsystem.

In eq.(1), S(0) denotes the last state of previous period.

Noticing that the existing communication devices in WSN do not employ the multi-voltage technology, we assume the voltage is a constant, denoted as V in the following.

IV. MODELING ENERGY CONSUMPTION FOR WORKING CLOCK DESIGN

In order to make clear, we use “state” in the description of hardware, and use “mode” to describe protocol in the following. Therefore, in the context of power management protocol, nodes in the wireless sensor network (WSN) is usually thought having four modes, i.e. transmitting, receiving, idle-listening, and sleeping. The first three modes happen while the node is active, and the sleeping mode is usually implemented by shutting down radio of node [2]. Measurements have shown that the power consumption while a node is in idle listening mode amounts to 50%-100% of the power consumption

required in the receiving mode [12]. Furthermore, typically, a node would spend a substantial fraction of the time in the idle listening mode. Therefore, idle listening has been considered as one of major source of energy waste in WSN, thus, low duty cycle scheme is widely employed in WSN.

However, when people talk about low duty cycle scheme in the synchronized sleeping schedule context, it is actually implied that two factors are involved, one is the ratio of active time to sleeping time, and another is the length of time frame of one working clock, i.e. the duty cycle and frequency of working clock of each nodes. In addition, because the nodes may be in different hardware states during the active period, and consume different amount of energy, duty cycle is not an accurate measurement of energy efficiency. Thus, we extend to the whole working clock, instead of being limited to the duty cycle.

A. Definition of Two Kinds of Working Clock

We use the linear network topology, where there are $N-1$ delay nodes between source node (denoted as S) and destination node (denoted as D), assume the distance between two adjacent nodes is R_{\max} , which is the maximum distance reachable with maximum transmitting power of device (figure 2(a)). We define an operation sequence for sending a data packet from source to destination as a transaction. Then, figure 2(b) and figure 2(c) present two working clock schemes for a transaction, which has same delay for one transaction, similar ratio of active interval to the length of time frame, but pretty different frequency of working clock. In figure 2(b) and 2(c), s , h , and d are used to denote the startup period, handshake period, and data forwarding period respectively. Assume handshake interval equal to the time of transmitting RTS and CTS, and, all nodes in h period are active for simplifying. In figure 2(b), data packet is forwarded one hop in each working clock. That means in each active interval, all nodes startup, handshake, and then data forwarding happens between two nodes while other nodes go to sleep. In Figure 2(c), the data packet is forwarded from source to destination via N hops in one working clock. That means at the beginning of a working clock all nodes startup and then repeat the h and d actions until the time when the data packet arrives the destination. During h , all nodes handshake with their neighbor nodes, and during d , two nodes do data forwarding while other nodes are idling.

For describing the protocols based on the above working clock definition exactly, we found that the conventional four modes (*transmitting*, *receiving*, *idlelistening*, and *sleeping*) are not enough. Thus we introduce two other modes, i.e. *idling*, and *waking*.

Here are the definitions of the six modes.

- ◊ *Transmitting/receiving*. Transmitting data or receiving data, including PHY overhead.
- ◊ *Idlelistening*. Listening, as to receive possible packet, or find opportunity to send data.
- ◊ *Sleeping*. Turn off Radio.
- ◊ *Idling*. Idling but not listening, while being aware of nothing will happen.
- ◊ *Waking*. Correspondent to the process of transferring from sleeping mode to idling mode.

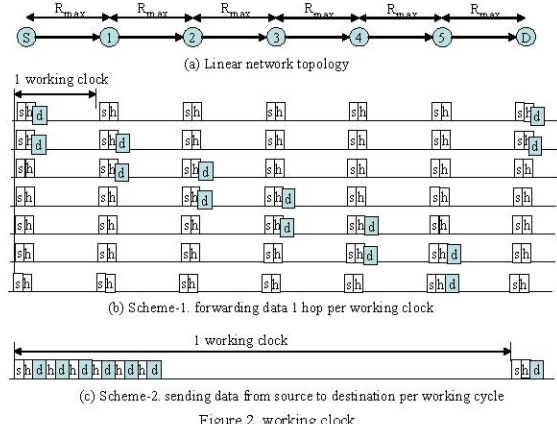


Figure 2. working clock

Moreover, for illustrating clearly, we define the following expressions. Assume

$$si \in \{\text{transmitting}, \text{receiving}, \text{idlelistening}, \text{sleeping}, \text{idling}, \text{waking}\}$$

Assume the basic operators are expressed in the following three types.

- ◊ $Tx_nd\{-si\}$ means transmitting node runs on the s mode.
- ◊ $Rx_nd\{-si\}$ means receiving node run on the s mode.
- ◊ $k\{-si\}$ means k nodes run on the s mode.

Assume *Operator-1* || *operator-2* represent *operator-1* is parallel with *operator-2*, i.e. starting at same time and ending at same time. Then, one transaction in *Scheme-1* (figure 2(b)) can be described in the pseudo code program as follows.

```

Begin
  Repeat for N times
    N-{waking}; /* s period
    Tx_nd-{transmitting RTS} || /* h period
    (N-1)-{receiving RTS};
    Rx_nd-{transmitting CTS} ||
    Tx_nd-{receiving CTS} ||
    (N-2)-{idlelistening};
    Tx_nd-{transmitting data packet} || /* d period
    Rx_nd-{receiving data packet} ||
    (N-2)-{sleeping};
    Rx_nd-{transmitting ACK} ||
    Tx_nd-{receiving ACK} ||
    (N-2)-{sleeping};
    N-{sleeping until start of next time frame};
End

```

Similarly, one transaction in *Scheme-2* (figure 2(c)) can be described as follows.

```

Begin
  N-{waking}; /* s period

```

```

Repeat N times
    Tx_nd-{transmitting RTS} ||      /* h period
    (N-1)-{Receiving RTS};
    Rx_nd-{transmitting CTS} ||
    Tx_nd-{receiving CTS} ||
    (N-2)-{idlelistening},
    Tx_nd-{transmitting data packet}|| /* d period
    Rx_nd-{receiving data packet} ||
    (N-2)-{idling};
    Rx_nd-{transmitting ACK} ||
    Tx_nd-{receiving ACK} ||
    (N-2)-{idling};
End
N-{sleeping until the start of next time frame}
End

```

B. Mapping to Communication Subsystem Model

Comparing the six modes (*transmitting, receiving,*

Table-2 Mapping schemes

Period	Nodes	Condition	State Sequence
Startup	(* ¹) N	If map <i>Sleeping</i> to <i>Power Off</i>	{ <i>Power Down; Power Save</i> }
		If map <i>Sleeping</i> to <i>Power Down</i>	{ <i>Power Save</i> }
		If map <i>Sleeping</i> to <i>Power Save</i>	None
Handshake	Tx_nd	None	{ <i>Tx(k₁ byte RTS); Rx(k₁ byte CTS)</i> }
	Rx_nd	None	{ <i>Rx(k₁ byte RTS); Tx(k₁ byte CTS)</i> }
	N-2	If map <i>Idlelistening</i> to <i>Rx</i>	{ <i>Rx(k₁ byte RTS); Rx(Waiting at Rx, until the end of handshake period)</i> }
Data forward	Tx_nd	None	{ <i>Tx(k₂ byte data); Rx(k₁ byte ACK)</i> }
	Rx_nd	None	{ <i>Rx(k₂ byte data); Tx(k₁ byte ACK)</i> }
	(* ¹) N-2	If map <i>Sleeping</i> to <i>Power Off</i>	{ <i>Power Save; Power Down; Power Off</i> }
		If map <i>Sleeping</i> to <i>Power Down</i>	{ <i>Power Save; Power Down</i> }
		If map <i>Sleeping</i> to <i>Power Save</i>	{ <i>Power Save</i> }
	(* ¹) N-2	If map <i>Idling</i> to <i>Power Down</i>	{ <i>Power Save; Power Down</i> }
		If map <i>Idling</i> to <i>Power Save</i>	{ <i>Power Save</i> }

(*¹) There are more than one mapping schemes. It is shown *sleeping* mode and *idling* mode of protocol can be mapped to more than one states of communication device.

C. Energy Consumption of Working Clock Schemes

Assume the distance from source to destination equals to N times of R_{\max} . Assume $N \times T_{frame} \leq T_{delay}$, where T_{frame} is the length of a working clock in *Scheme-1*, T_{delay} is the delay constraint from source to destination. Then, length of working clock in *Scheme-2* is $N \times T_{frame}$.

Based on the pseudo code programs and equation (1), for *Scheme-1*, we derive the following total energy consumption of N nodes in one transaction.

$$E_D = \sum_{i=1}^N \sum_{j=1}^N \left(\sum_{k=1}^{m_j} T_{S(i,j,k)} \times I_{S(i,j,k)} + \sum_{k=0}^{m_j-1} T_{S(i,j,k) \rightarrow S(i,j,k+1)} \times I_{S(i,j,k) \rightarrow S(i,j,k+1)} \right) \times V \quad (2)$$

Where, $N+1$ is the total number of node, N is the total number of working cycle; i is the index of working

idlelistening, sleeping, idling, and waking) in the description of working clock schemes with the states of communication subsystem (*Power off, Power down, Power save, Rx, and Tx*), we found that there are more than one mapping schemes. Later, we will show that optimized mapping scheme is determined by both of the device parameters and the application requirement. Table-2 presents examples of the implementation of *Scheme-1* and *Scheme-2* by mapping the working clock schemes to the communication subsystem model presented in section 3.A and 3.B. Here, assume $\{s_1; s_2\}$ denote state sequence.

cycles and j is the index of nodes; m_{ij} is the total number of states of the j th node in the i th working cycle. Assume T_{s1} and T_{s2} denote the duration of sleeping, t denotes $1/bit_rate$. Assume the length of control packet is same, denoted as k_1 (byte), then, the time for transmitting/receiving RTS/CTS/ACK is $8k_1t$. Assume the length of data packet is same, denoted as k_2 (byte), then, the time for Transmitting/Receiving a data packet is $8k_2t$. Mapping sleeping mode to *Power Off* state, the state sequence of j th node at i th cycle, $S(i,j)$,

$$S(i,j) = \begin{cases} (\text{Power_down}, \text{Power_save}, \text{Tx}(k_1), \text{Rx}(k_1), \text{Tx}(k_2), \text{Rx}(k_2), \text{Power_off}(T_{s1})), i=j \\ (\text{Power_down}, \text{Power_save}, \text{Rx}(k_1), \text{Tx}(k_1), \text{Rx}(k_2), \text{Tx}(k_1), \text{Power_off}(T_{s1})), i=j+1 \\ (\text{Power_down}, \text{Power_save}, \text{Rx}(k_1), \text{Rx}(k_1), \text{Power_off}(T_{s2})), \text{other} \end{cases}$$

Where,

$$T_{s2} = T_{frame} - T_{off_down} - T_{down_save} - T_{save_tx} - 8k_1t - T_{tx_rx} - 8k_1t$$

$$T_{s1} = T_{s2} - T_{rx_tx} - 8k_2t - T_{tx_rx} - 8k_1t$$

Similarly, the state sequence of mapping sleeping mode to *Power Down* or *Power Save* state of communication subsystem can be derived.

For *Scheme-2*, we can derive the total energy consumption of N nodes in one transaction in the similar way, i.e.

$$E_D = \sum_{i=1}^{N+1} (E_s + E_T) \quad (3)$$

where,

$$E_S = (\sum_{k=1}^{m_i} T_{S(i,k)} \times I_{S(i,k)} + \sum_{k=1}^{m_j-1} T_{S(i,k) \rightarrow S(i,k+1)} \times I_{S(i,k) \rightarrow S(i,k+1)}) \times V$$

$$E_T = \sum_{j=1}^N (\sum_{k=1}^{m_j} T_{S(i,j,k)} \times I_{S(i,j,k)} + \sum_{k=0}^{m_j-1} T_{S(i,j,k) \rightarrow S(i,j,k+1)} \times I_{S(i,j,k) \rightarrow S(i,j,k+1)}) \times V$$

The total number of node is $N+1$, the total number of hop is N ; i is the index of nodes and j is the index of hop; m_{ij} is the total number of states of the i th node in the j th hop. Assume T_s denotes the duration of sleeping, E_S is the energy consumed during the start-up period, E_T is the energy consumed during the communication for one transaction. The state sequence for mapping sleeping mode to *Power Off* state is following.

$$\forall i, S(i) = \{\text{Power_off}, \text{Power_down}, \text{Power_save}\}$$

$$S(i, j,) = \begin{cases} \{Tx(k_1), Rx(k_1), Tx(k_2), Rx(k_1)\}, i = j, j \leq N \\ \{Rx(k_1), Tx(k_1), Rx(k_2), Tx(k_1)\}, i = j + 1, j \leq N \\ \{\text{Power_off}(T_s)\}, j = N + 1 \\ \{\text{Power_save}(8(k_2 + 3k_1)t)\}, \text{other} \end{cases}$$

Where,

$$T_s = N \times T_{frame} - T_{off_down} - T_{down_save}$$

$$- N \times (T_{save_tx} + 8k_1t + T_{tx_rx} + 8k_1t + T_{rx_tx} + 8k_2t + T_{tx_rx} + 8k_1t)$$

Similarly, the state sequence of mapping sleeping mode to *Power Down* or *Power Save* state of communication subsystem can be derived.

D. Validation

We validated the CSECM by the measurements on the realistic devices based wireless sensor networks. The objective of the experiments is to present a method to extract the parameters of CSECM, so as to prove the validation of CSECM.

D.1 Experiment Setting

The oscilloscope (Tektronix TDS7404B) was used to measure. The oscilloscope provides a 20 GHz sampling resolution. All data was logged digitally for analysis later. For measuring the dynamic feature of current accurately, a current probe (TCP202) is used.

For the experiment on sleeping scheduling, a linear network topology is used, where there are four delay nodes between S and D (Figure2a). CC1000 is used as communication subsystem, bit-rate is 19.2kbps, transmitting power is 10dbm, and crystal is

14.75MHz. For *Scheme-1*, the behavior of sending and receiving in one transaction is measured separately; for *Scheme-2*, the behavior of sending, relaying and receiving in one transaction is measured separately. A pseudo-TDMA is used to repeat the behavior of one transaction, as to support the measurement separated. For the experiments on devices, CC1000 and CC2420 are used as communication subsystem, respectively.

D.2 Result and Analysis

Figure 3(a) is the waveform in the transmitting side of *Scheme-1*, using *sample mode* of oscilloscope as capture mode. Furthermore, for showing the transition more clearly, *Hi-Res mode* of oscilloscope is used for capturing the waveform of transitions. Figure 3(b) and 3(c) show the waveform of CC1000 and CC2420 during transition from *Power Off* to *Power Down*. Meanwhile, CPU is active. Thus, I_{off_down} is the difference between the captured current shown in waveform and the current consumed in CPU, i.e. 8mA and 7.65mA, respectively. Figure 3(d) and 3(e) show the typical transition behaviors of CC1000 and CC2420, respectively.

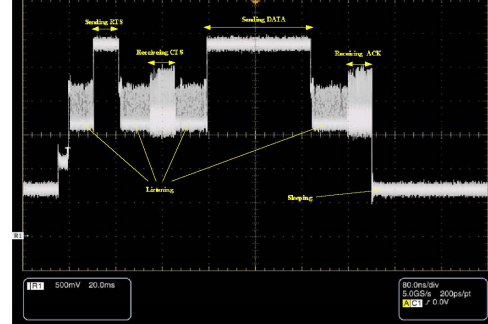


Fig. 3(a) CC1000, Waveform in transmitting side

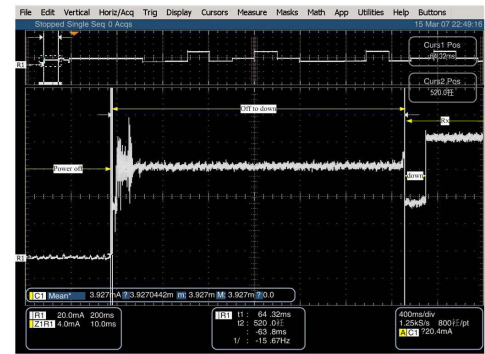


Fig. 3(b) CC1000, Waveform in transition from *Power Off* to *Power Down*, $I_{off_down} = 4.09\text{mA}$, $T_{off_down} = 63.8\text{ms}$

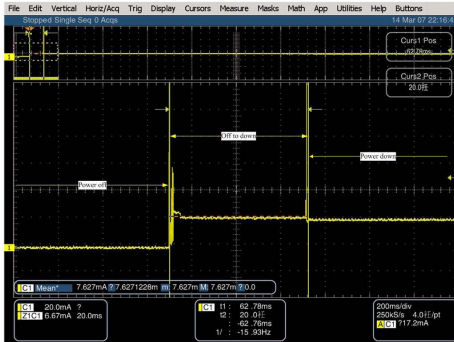


Fig. 3(c) CC2420, Waveform in transition from *Power Off* to *Power Down*, $I_{\text{off_down}}=0.62\text{mA}$, $T_{\text{off_down}}=62.76\text{ms}$

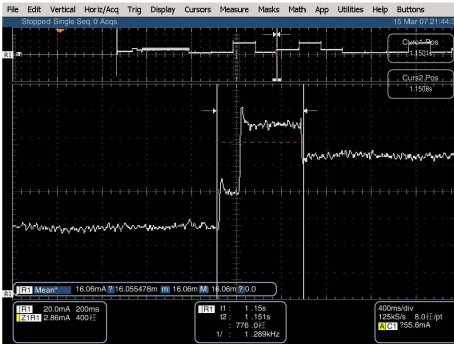


Fig. 3(d) CC1000, Waveform in transition from *Power Save* to *Rx*, $I_{\text{save_rx}}=9.78\text{mA}$, $T_{\text{save_rx}}=0.776\text{ms}$

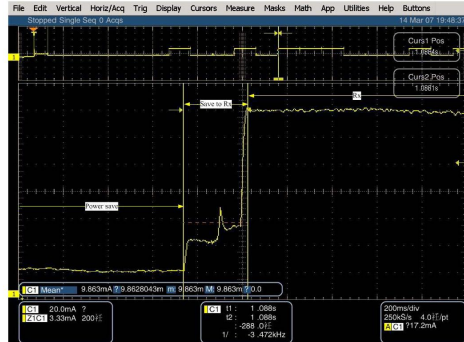


Fig. 3(e) CC2420, Waveform in transition from *Power Save* to *Rx*, $I_{\text{save_tx}}=9.863\text{mA}$, $T_{\text{save_tx}}=0.288\text{ms}$

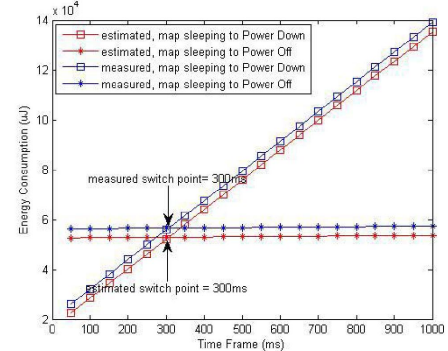


Fig. 3(f) CC1000, Estimation vs. Measurement

Table-3 comparing data from datasheet and the data measured

Curr. para.	Interval para.	CC1000 measurement		CC1000 estimation		CC2420 measurement		CC2420 estimation		Datasheet-based estimation of current during transition
		mA ^(*)1)	ms	mA ^(*)1)	ms	mA ^(*)3)	ms	mA ^(*)3)	ms	
I_{off}	T_{off}	0.01		0.01		0.001		0.001		
I_{down}	T_{down}	1.1		1.1		0.02		0.02		
I_{save}	T_{save}	2.37		1.86		0.42		0.426		
I_{rx}	T_{rx}	10.45		10.3 ^(*)2)		19.93		19.7		
I_{tx}	T_{tx}	30.71		27.7		16.73		17.4		
$I_{\text{off down}}$	$T_{\text{off down}}$	5.09	63.8	5.09	63.8	0.62	62.76	0.62	62.76	None
$I_{\text{down save}}$	$T_{\text{down save}}$	3.22	2.4	1.86	2.2	1.47	2.424	0.426	0.96	$I_{\text{down save}} = I_{\text{save}}$
$I_{\text{save rx}}$	$T_{\text{save rx}}$	10.78	0.776	6.08	0.25	2.07	0.288	10.02	0.192	$I_{\text{save rx}} = (I_{\text{save}} + I_{\text{rx}})/2$
$I_{\text{save tx}}$	$T_{\text{save tx}}$	12.47	0.76	14.28	0.27	7.06	0.220	8.92	0.192	$I_{\text{save rx}} = (I_{\text{save}} + I_{\text{tx}})/2$
$I_{\text{tx rx}}$	$T_{\text{tx rx}}$	23.72	0.7	19.0	0.25	9.11	0.292	18.55	0.192	$I_{\text{tx rx}} = (I_{\text{tx}} + I_{\text{rx}})/2$
$I_{\text{rx tx}}$	$T_{\text{rx tx}}$	14.06	0.9	19.0	0.27	6.81	0.220	18.55	0.192	$I_{\text{rx tx}} = (I_{\text{rx}} + I_{\text{tx}})/2$

(*)¹⁾ including the current consumed by VR on PCB board.

(*)²⁾ CC1000 is in normal current setting.

(*)³⁾ VR on chip is enabled

Table-3 presents the measured data of CC1000 and CC2420 devices entirely. The measured current is the average of current in the period. The estimation is extracted from the datasheet [14] [15]. The estimated current during steady states and the estimated time of each transition come from datasheet directly. However, the datasheets do not present the current during each transition. From the measurement we found that, because the register and RAM programming will be lost while the device goes the state of *Power Off*, the current and the interval during the transition from *Power Off* to *Power Down* not only depends on the

device, but also depends on the initial processes of the devices. Thus, we suggest applying the measured $I_{\text{off_down}}$ to CSECM. In another word, in order to establish an energy consumption model for a specific device, the $I_{\text{off_down}}$ should come from measurement. For other transitions, we found that the process of transition highly depends on the implementation of device, e.g. figure 3(d) and figure 3(e). Figure 3(f) shows the comparison of the estimated result with the measured value based on *Scheme-1* of working clock design, while mapping sleeping mode to *Power Off*, *Power Down*, respectively. It is shown that the switch

points in both estimation and measurement are almost same, even the energy consumption in measurement is little higher than that estimated. Thus, we conclude that most of parameters can be estimated based on datasheets, except the parameter of the transition from *Power Off* to *Power Down*. The feature makes CSECM easy to use.

V. CRITERIA FOR ENERGY EFFICIENT SLEEPING SCHEDULING

From the model above, we are going to derive some criteria for upper layer protocol design. The first one is the criterion for selecting mapping scheme, which is used to answer the question “what state of device should be used to implement *sleeping* mode for a given frequency of working clock”. The second one is the criterion for selecting working clock frequency, which is used to answer the question “what kind of working clock scheme, more specifically, the frequency of working clock should be used for a given length of control package k_1 and data package k_2 ?”

A. Criterion for selecting mapping scheme

A.1 Analysis

Assume *Scheme-1* is used. From equation (2) the difference between mapping *sleeping* to *Power Off* with mapping *sleeping* to *Power Down* is following.

$$Y = N^2 T_{off_down} \times I_{off_down} \times V + N^2 \times (T_{sl_off} \times I_{off} \times V - T_{sl_down} \times I_{down} \times V) - 2N \times (T_{rx_tx} + 8k_2 t + T_{tx_rx} + 8k_1 t) \times (I_{off} \times V - I_{down} \times V)$$

Let $Y < 0$, then.

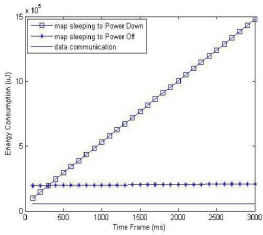


Fig. 4(a). CC1000, Assume $k_1=19$, $k_2=133$, $N=12$, bit-rate = 76Kbps, $V=3.0V$

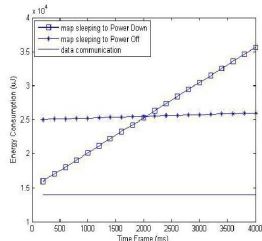


Fig. 4(b). CC2420, $k_1=19$, $k_2=133$, $N=12$, bit-rate = 250Kbps, $V=1.8V$

$$\begin{aligned} & N(I_{down} - I_{off}) \times (T_{frame} - T_{down_save} - T_{save_tx} - T_{tx_rx} - 16k_1 t) \\ & - N(I_{off_down} - I_{off}) \times T_{off_down} \\ & - 2(I_{down} - I_{off}) \times (T_{rx_tx} + 8k_2 t + T_{tx_rx} + 8k_1 t) > 0 \end{aligned}$$

Because $2(I_{down} - I_{off}) \times (T_{rx_tx} + 8k_2 t + T_{tx_rx} + 8k_1 t)$ is much smaller than other two parts, we can obtain an approximation as following.

$$\begin{aligned} & (I_{down} - I_{off}) \times (T_{frame} - T_{down_save} - T_{save_tx} - T_{tx_rx} - 16k_1 t) \quad (4) \\ & > (I_{off_down} - I_{off}) \times T_{off_down} \end{aligned}$$

Assume T_{frame_sw} denote the value which makes $Y=0$, then equation (4) means that, for each device,

- ❖ When $T_{frame} < T_{frame_sw}$, mapping *sleeping* mode to *Power Down* state is more energy efficient; and when T_{frame} increases and is greater than T_{frame_sw} , mapping *sleeping* mode to *Power Off* state will become more energy efficient than mapping to *Power Down* state;
- ❖ The network scale expressed by N has almost no impact on the switch point T_{frame_sw} .
- ❖ The length of data packet (k_2) is almost irrelevant with the value of T_{frame_sw} .

Similarly, the criterion for mapping *sleeping* mode to *Power Save* state can be found. However, if using the parameter values of current communication device (e.g. parameters of CC1000 and CC2420 listed in Table-3), it will be found that mapping *sleeping* mode to *Power Save* state is usually not energy efficient.

A.2 Case study

In this section, our objective is to understand the impact of parameters of realistic devices. We use the parameters of CC1000 and CC2420 from measurement (Table-3) in the following analysis.

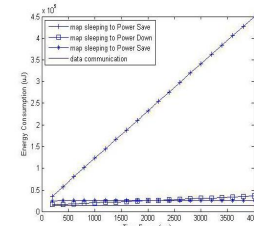


Fig. 4(c) CC2420. Comparing with the scheme of mapping sleeping to *Power Save*. $k_1=19$, $k_2=133$, $N=12$, bit-rate = 250Kbps, $V=1.8V$

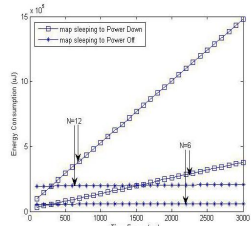


Fig. 4(d) CC1000. Impact of N . $k_1=19$, $k_2=133$, $N=6, 12$, bit-rate = 76Kbps, $V=3.0V$

Applying the parameters in Table-3 to equation (2), then we found the following.

- ❖ For different devices, the switch point T_{frame_sw} changes dramatically, e.g. for CC1000, while T_{frame} is less than about 300ms (Figure 4(a)), mapping *sleeping* mode to *Power Down* state is

more energy efficient; but for CC2420, the switch point equals to 2000ms (Figure 4(b)). The main reason is that, comparing with CC1000, the VR of CC2420 consumes much less current, i.e. 1.1mA in CC1000 vs. 0.02mA in CC2420.

- ❖ Figure 4(c) shows mapping *sleeping* mode to

- Power Save* state is very energy consumed, and the energy inefficiency will significant increase while the T_{frame} increase. It is because the energy consumption in the *Power Save* state of current devices is much larger than the sum of energy consumption for sleeping in *Power Down* state plus the energy consumption for waking up XOSC and its associated circuit.
- ❖ Figure 4(d) shows the network scale (i.e. N) has almost no impact on switch point, i.e. 300ms.

As we mentioned in section 2, ref [9] only considers four states of device (*shutdown, idle, transmit, and receive*), and thus maps *sleeping mode* to *shutdown*, i.e. *Power Down* in CSECM, in which clock is turn off but the voltage regulator (VR) remains on. The analysis and figure 4(b) show that the algorithm is less energy efficient than that implemented by mapping *sleeping mode* to *Power Off* state for CC2420 while the time frame is large than 2000ms, which is always the case in WSN application. The example shows that it is possible to derive criteria for upper layer protocol design based on CSECM.

B. Criterion for selecting working clock frequency

B.1 Analysis

Assume mapping *sleeping mode* to *Power Off* state, from equation (2) and (3), the difference between *Scheme-1* and *Scheme-2* is derived, denoted as Z . And let $Z < 0$, then,

$$(I_{off} + I_{save}) \times (T_{rx_tx} + 8k_2 t) \\ > \frac{N-1}{N-2} ((I_{off_down} + I_{off}) \times T_{off_down} + (I_{down_save} + I_{off}) \times T_{down_save})$$

Because T_{rx_tx} is much smaller than $8k_2 t$, then the approximation is following.

$$k_2 > \frac{N-1}{N-2} \times \frac{(I_{off_down} + I_{off}) \times T_{off_down} + (I_{down_save} + I_{off}) \times T_{down_save}}{(I_{off} + I_{save}) \times 8t} \quad (5)$$

We use K_2 denotes the value of k_2 which makes

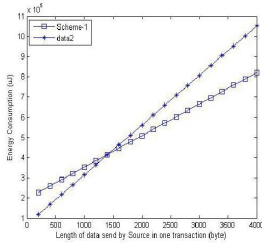


Fig. 5(a) CC1000, Mapping *sleeping mode* to *Power Off*. $k_1=19$, $N=12$, bit rate = 76Kbps, $V=3.0V$

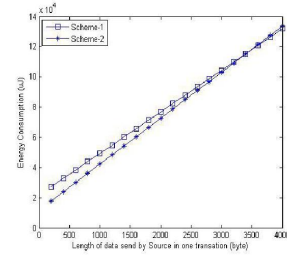


Fig. 5(b) CC2420, Mapping *sleeping mode* to *Power Off* state. $k_1=19$, $N=12$, bit rate = 250Kbps, $V=1.8V$

$Z=0$. Then, equation (5) means that, for each device,

- ❖ When the length of data packet is relatively small ($k_2 < K_2$), the *Scheme-2* is more energy efficient than *Scheme-1*; and when k_2 is greater than K_2 and increase continually, *Scheme-1* will become more energy efficient than *Scheme-2*;
- ❖ The network scale expressed by N has no significant impact on the switch point K_2 ;
- ❖ If the other parameters are fixed, K_2 increases while the bit rate increases.

B.2 Case study

Applying the same parameters value listed in Table-3 to equation (2) and equation (3), and let $T_{frame}=5000ms$, we found the following.

- ❖ For different devices, by mapping *sleeping mode* to *Power Off* state, the switch point K_2 is pretty different. For example, the K_2 of CC1000 is about 1400byte (figure 5(a)); but the K_2 of CC2420 is about 3400byte (figure 5(b)). It means that for the application characterized by small data packet communication, which is a typical scenario in WSN, *Scheme-2* is more energy efficient. In addition, more important, it shows that if the length of data packet is longer, e.g. 2048byte, the more energy efficient scheme may be *Scheme-1* (figure 5(a)) or *Scheme-2* (figure 5(b)), depending on what kind of device is used.
- ❖ For the same device, by mapping *sleeping mode* to different state, the switch point K_2 is also changing dramatically. For example, while mapping *sleeping mode* to *Power Down* state (figure 5(c)), instead of mapping to *Power Off* state (figure 5(a)), it is shown that *Scheme-2* is never more energy efficient than *Scheme-1*.
- ❖ Figure 5(d) shows the network scale (i.e. N) has a little impact on switch point K_2 .

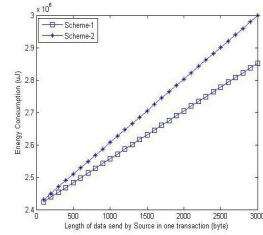


Fig. 5(c) CC1000, Mapping *sleeping mode* to *Power Down*. $k_1=19$, $N=12$, 76Kbps, $V=3.0V$

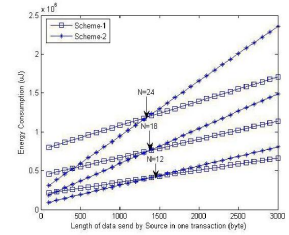


Fig. 5(d) CC1000. Impact of N . Mapping *sleeping mode* to *Power Off*. $k_1=19$, $N=12, 18, 24$, 76Kbps, $V=3.0V$

VI. CONCLUSION

The energy consumption of communication subsystem in the wireless sensor network devices is divided into two parts, one is that related to an adjustable transmission power, and another is related to the power consumption of the remaining circuit. In this paper, we show that the second part of energy consumption varies significantly from state to state of a device and among various types of real WSN devices. Moreover, we show that, in terms of energy consumption, there is a gap between the real device characteristics and the device features typically modeled by designers of energy-aware protocols for upper layers of WSN (e.g. there is usually more than one hardware state corresponding to sleeping mode in hardware implementations of power management.)

The main contribution of this paper includes: (1) from the view of energy consumption, generalizing the communication subsystem in wireless sensor network devices, which reflects the actual hardware architecture and state machine of most WSN devices; (2) proposing an energy consumption model for the communication subsystem (CSECM) which is validated by experimental measurements with real WSN devices using realistic CSECM parameters simply extracted primarily from the device hardware specification; (3) presenting a methodology which uses the CSECM to evaluate various synchronized sleeping schedule protocols as an example of energy efficient upper layer design.

The application of CSECM shows that the model, especially its parameterization, has significant impact on evaluating energy efficiency of different working clock designs and which represents a significant improvement over existing models that are typically used. Taking ref. [9] as an example, it is shown that, based on the parameters measured in this paper, the algorithm in ref. [9] will increase its energy efficiency if taking *Power Off* into energy consumption model and mapping *sleeping* mode to *Power Off* state of device. The application of CSECM demonstrates that it is possible to derive criteria for upper layer protocol design based on CSECM. It also shows that the performance of an energy-aware algorithm/protocol depends on not only the application characteristics, e.g. length of sending data, but also the device features identified in this paper. Therefore, CSECM can be used to guide the choices in many different sides of the design space, e.g. WSN application system design, hardware design, WSN simulator design, upper layer protocol design and evaluation.

In the next step, we are going to study the impact of CSECM on the other protocols, such as MAC protocol, routing protocol, according to the

methodology proposed in this paper. In addition, we are going to establish the energy consumption model for the other subsystems in the sensor network device, such as processing module, sensing module, and add them into the analysis of energy efficiency.

REFERENCE

- [1] Chunlong Guo, Lizhi Charlie Zhong, Jan. M. Rabaey, Low Power Distributed MAC for Ad Hoc Sensor Radio Network, GLOBECOM2001
- [2] Wei Ye, John Heidemann, Deborah Estrin, Medium access control with coordinated adaptive sleeping for wireless sensor networks, IEEE/ACM Transactions on Networking (TON), Volume 12 Issue 3, June 2004
- [3] Qin Wang, Zygmont J. Haas, BASS: an Adaptive Sleeping Scheme for Wireless Sensor Network with Bursty Arrival, IWCMC2006
- [4] Ivan Stojmenovic and Xu Lin, Power-Aware Localized Routing in Wireless Networks, IEEE Trans. On Parallel and Distributed System, Vol. 12, No. 11, NOV. 2001
- [5] Qin Wang, Mark Hempstead and Woodward Yang, A Realistic Power Consumption Model for Wireless Sensor Network Devices, SECON2006
- [6] W. R. Heinzelman, A. P. Chandrakasan, and H. Balakrishnan, An application specific protocol architecture for wireless microsensor networks, IEEE trans. Wireless Communications, Oct. 2002
- [7] Cintia B. Margi, Katia Obraczka, Instrumenting network simulators for evaluating energy consumption in power-aware ad-hoc network protocols, MASCOT'04
- [8] Ivan Howitt, Rogelio Neto, Jing Wang, and James M. Conrad, Extended Energy Model for the Low Rate WPAN, MASS'05
- [9] Bruno Bougard, Francky Catthoor, Denis C. Daly, Anantha Chandrakasan, Wim Dehaene, Energy Efficiency of the IEEE 802.15.4 Standard in Dense Wireless Micro-sensor Networks: Modeling and Perspectives, DATE2005.
- [10] Pilsoon Choi, el., An Experimental Coin-Sized Radio for Extremely Low-Power WPAN (IEEE 802.15.4) Application at 2.4GHz, IEEE Journal of Solid-State Circuits, Vol. 38, No. 12, Dec. 2003
- [11] Ben W. Cook, Alyosha Molnar, and Kristofer S. J. Pister, Low Power RD Design for Sensor Networks, IEEE Radio Frequency Integrated Circuit Symposium, 2005
- [12] M. stemm, R. H. Katz, "Measuring and reducing energy consumption of network interfaces in hand-held devices", IEICE Trans. Communication. pp1125-1131, Aug. 1997
- [13] Atmega128/128L, datasheet
- [14] Chipcon, SmartRF CC1000 Single Chip Very Low Power RF Transceiver
- [15] Chipcon, SmartRF CC2420, 2.4GHz IEEE 802.15.4/ZigBee-ready RF Transceiver